Sensors and Materials, Vol. 17, No. 2 (2005) 087–095
MYU Tokyo

S & M 0589

Multifunctional Probe for Chemical Stimulation and Neural Signal Recording

Kyo-in Koo, Jung-Min Lim, Seung-Joon Paik, Jaehong Park, Sangwon Byun, Ahra Lee, Sungil Park, Taeyong Song, HyunMin Choi, Myoung-Jun Jeong and Dong-il "Dan" Cho*

School of Electrical Engineering and Computer Science, Seoul National University, San 56-1, Shinlim-dong, Kwanak-gu, Seoul 151-742, South Korea

(Received April 10, 2004; accepted November 16, 2004)

Key words: microchannel, microelectrode, low impedance, neural probe

This paper presents a single-unit neural probe which functions both as a neural signal recorder and a chemical stimulator. The single-unit neural probe contains in-plane shanks with buried microchannels and low-impedance microelectrodes that are fabricated using the roughened polysilicon process. The fabricated neural probe has three 3-mm-long shanks with 10-μm-diameter microchannels, and six 30 μm × 30 μm gold microelectrodes per shank. The impedance magnitude and phase shift of the microelectrodes are 317 kΩ / 900 μm^2 and –56.2° at 1 kHz, respectively.

1. Introduction

Various micromachined neural probes have been developed for studying interactions between neurons and neural prostheses.[1–6] These neural probes are biocompatible, minimally invasive, and reproducible in a batch fabrication process. However, most of the previous works investigated neural systems utilizing a single method of either an electrical measurement or a drug delivery. While the electrical charge distributions and potentials of the probe are important factors for determining neuronal activity, it is well known that the complex biochemical reactions between the neural probe and the cells are the major factors that determine the functionality of the probe. Thus, in order to obtain a better understanding of neuronal behavior, we now seek to deliver the proper chemicals to a highly localized area of the neural tissue while monitoring its responses to the chemicals *in vivo*. Chen and Wise previously integrated microelectrodes and microchannels in a single probe unit using a (100) oriented silicon substrate.[7,8] However, due to the anisotropic wet etching used for

*Corresponding author, e-mail address: dicho@asri.snu.ac.kr

the formation of microchannels, the microchannels were aligned in the <100> direction, a few microns below the top silicon surface.

This paper describes a new method of fabricating a single-unit neural probe integrated with a drug delivery system and a neural signal recording system. The fabricated neural probe chemically stimulates the neuron via the buried microchannels and records the neuron's responses with the microelectrodes. The shanks of the neural probe are in-plane. The buried microchannels are fabricated by an isotropic dry etch. Therefore, the shank length of the probe is longer than that of the out-of-plane-type probe, and there is no limitation on the direction and depth of the microchannels.[1,2,5] Fabricated microelectrodes are also formed on the roughened polysilicon film to achieve low impedance.[3,4]

2. Design

In order to prevent the displacement of a neural probe from its initial position, barbs are proposed as shown in Fig. 1. Considering the penetration ability and the mechanical stability of the shank, the shape, length, width, and thickness of the shanks are designed.[5]

The body of the probe is 7.5 mm long, 4 mm wide, and 540 μm thick, and contains a 2 mm × 2 mm × 100 μm reservoir. The probe has three shanks, and each shank has five or six microelectrodes. The length of each shank is 3000 μm. The microelectrodes are 30 μm × 30 μm rectangles. Their dimensions are determined by considering the size of a neural cell. At the wall of a shank, microchannels are positioned 40 μm away from the microelectrodes (Fig. 2(b)). The diameter of the microchannels is 10 μm (Fig. 2(d)).

3. Fabrication

Paik *et al.* have previously reported a method for fabricating hollow single-crystal-silicon microneedles using anisotropic and isotropic dry etching, trench-refilling, and release dry etching.[1,2] Similarly, Chen *et al.* fabricated buried microchannels in a p-type (100)-oriented silicon substrate using anisotropic wet etching and sealed the surface by deposition of a low pressure chemical vapor deposition (LPCVD) thin film. Briefly, a

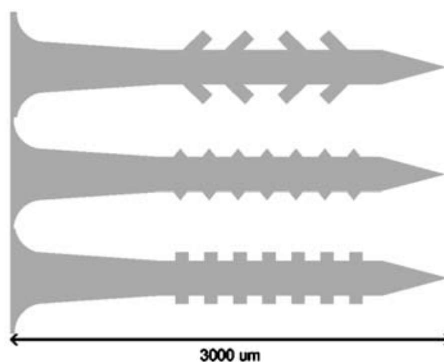

Fig. 1. Design variation of shanks: zigzags, triangular and rectangular shapes.

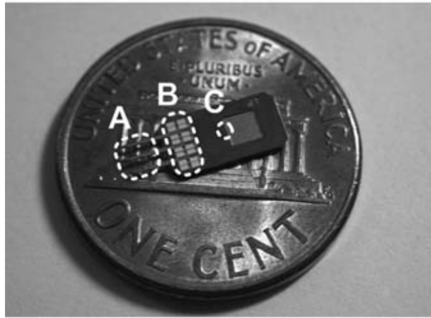

(a) Picture of device.

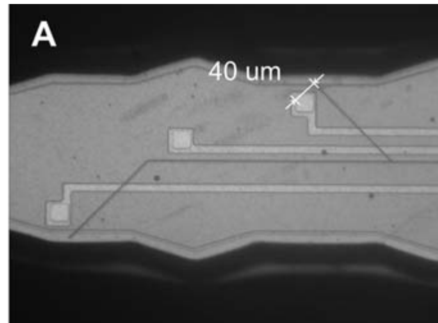

(b) Magnified picture of shank: The center of the microelectrodes is 40 µm away from the end of the microchannels on a spike-shaped shank. (Part A in Fig. 2(a)).

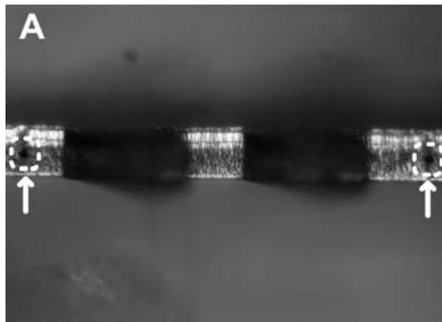

(c) Magnified picture of outlets of microchannels on the side wall of the shank (Part A in Fig. 2(a)).

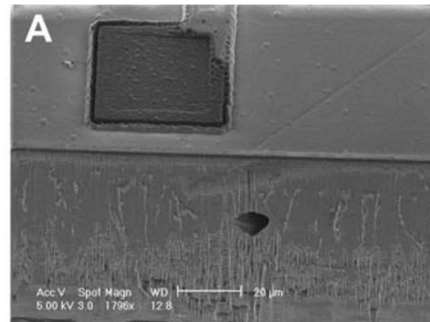

(d) SEM image of the microchannel and the microelectrode on the shank (Part A in Fig. 2(a)).

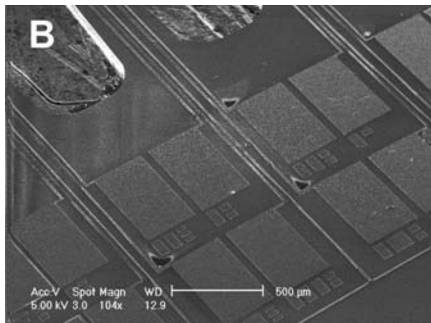

(e) SEM image of bonding pads on the body (Part B Fig. 2(a)).

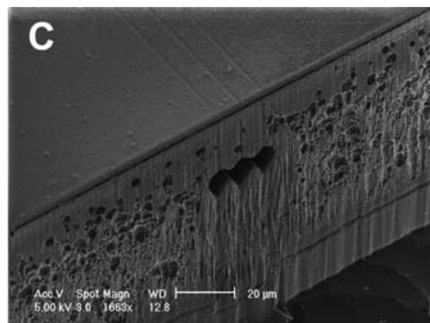

(f) SEM image of microchannels at the reservoir (Part C in Fig. 2(a)).

Fig. 2. Pictures of device.

heavily boron-doped silicon layer was used as an etch mask, and an opening perpendicular to the (100) direction was cut through this layout to expose the (100) plane.[7,8] Then, the mask was undercut by subsequent wet etching to form continuous flow microchannels. However, due to the anisotropic wet etching, the microchannels must be aligned in the (110) direction, and the microchannels were located only a few microns below the top silicon surface.

In this study, the modified microchannel fabrication process is developed to overcome the limitations of Chen's process.[1,2] The fabrication process is shown in Fig. 3. Although a (100)-oriented silicon substrate is used, the fabrication process can also be applied to any orientated wafer. The microchannel fabrication process is shown in Figs. 3 (a)–3(e). An oxide layer is used as an etch mask. Then, microchannels are fabricated using anisotropic dry etching and sidewall passivation with thermal oxide or LPCVD nitride film, isotropic dry etching with a SF_6 plasma, and trench-refilling with LPCVD poly-silicon film. Briefly, the anisotropic dry etching process defines the depth of the microchannels below the top silicon surface, which can range from a few microns to tens of microns, or even deeper. The sidewall passivation prevents the trench from being etched during the subsequent isotropic dry etching process. Then, the isotropic dry etching defines the diameter of the microchannel. Because of the isotropic dry etching process for microchannels, the direction of the microchannels can be oriented to any crystallographic direction in-plane, which is an advantage over Chen's process.

Previous studies have reported various methods of reducing the electrical impedances.[7–23] Several approaches such as the enlargement of physical dimensions were implemented to minimize the impedance by considering the signal-to-noise ratio, process steps, cell size and positioning.

We have previously reported a simple method of fabricating low-impedance electrodes which is compatible with the generic CMOS process and batch process.[3,4] Since phosphorus atoms in a phosphosilicate glass (PSG) film disturb the nucleation of polysilicon during LPCVD, the density of polysilicon nuclei becomes low. Thus, the grains of polysilicon become larger.[24,25] In this work, this roughened surface is utilized to decrease the electrical impedance. The detailed process is presented in Figs. 3(f)–3(h). Briefly, a 12 wt% PSG film is deposited in an atmospheric pressure CVD (APCVD) reactor. Then, a 2-μm-thick polysilicon film is deposited using a horizontal hotwall LPCVD reactor with the pressure fixed at 300 mTorr and the SiH_4 flow rate fixed at 60 sccm at 625°C. This condition makes polysilicon film roughened as expected. The uniformity of the polysilicon film is within ±5% of the 2 μm thickness across the wafer.[25–27] After forming the roughened LPCVD polysilicon film, titanium and gold films are deposited using a sputtering system (MHS-1500, Moohan, Korea). After successful patterning of the microelectrodes, a 300-nm-thick plasma-enhanced CVD (PECVD) oxide film is deposited to insulate the microelectrodes, and the recording sites and bonding pads are opened.

4. Results

A picture of the entire device is shown in Fig. 2(a). Briefly, part A in Fig. 2(a) shows three shanks of the device which contain the microelectrodes and the outlets of microchannels. Part B in Fig. 2(a) shows the metal pads for wire bonding to a printed

(a) Anisotropic etching

(b) CVD oxide film deposition

(c) Bottom oxide film etching

(d) Isotropic etching

(e) Gap filling

(f) PSG and polysilicon deposition

(g) Defining microelectrode shape

(h) Isolation layer deposition

(i) Front-side etching

(j) Back-side etching

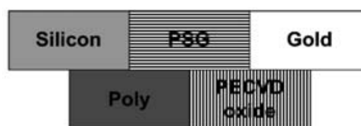

Material index

Fig. 3. Process flow.

circuit board (PCB). Part C in Fig. 2(a) shows the inlet of the the microchannels and the reservoir. The center of the microelectrodes is 40 μm from the end of microchannels on a spike-shaped shank, as shown Fig. 2(b). Outlets of the microchannels at the sidewall of the shank are shown in Figs. 2(c) and 2(d). The diameter of the microchannels is approximately 10 μm .

As expected, microelectrodes fabricated on the roughened polysilicon are rougher than those fabricated on the nitride film. Atomic force microscopy (AFM, SSM SRP 150, PSI, Korea) images show the gold microelectrode surfaces on nitride film and on the roughened poly-silicon film in Fig. 4. The microelectrode formation on silicon has an average roughness of 2.49 nm and the root-mean-square roughness of 3.10 nm. An average roughness of 26.77 nm is measured for the microelectrode on the roughened polysilicon film and the root-mean-square roughness is 34.08 nm.

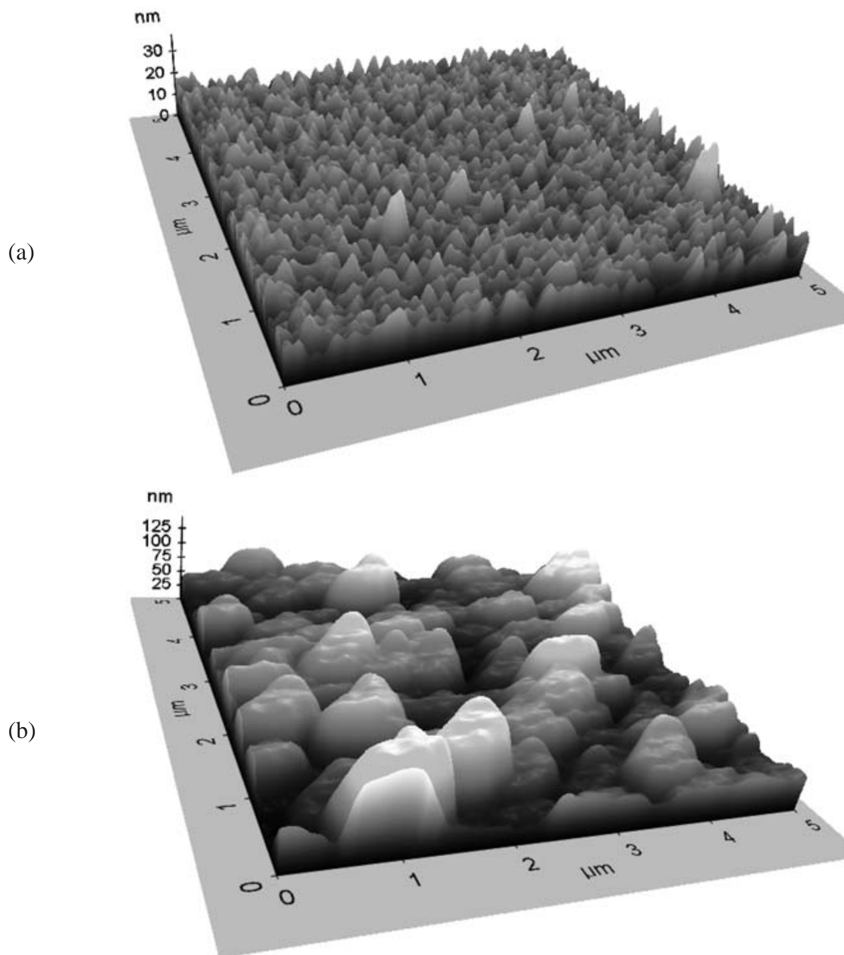

Fig. 4. AFM images of gold microelectrode surface. (a) Smooth surface of the gold electrode on silicon with an average roughness of 2.49 nm and with a root-mean-square roughness of 3.10 nm. (b) Roughened surface of the gold electrode on polysilicon with an average roughness of 26.77 nm and a root-mean-square roughness of 34.08 nm.

The fabricated device is mounted onto a printed circuit board (PCB) using epoxy resin, and followed by bonding pads and metal lines with gold wires 50 µm in diameter. Using this device, electrical impedance is measured with an impedance analyzer (ZAHNER-electrik IM6e). A large Ag/AgCl electrode is used as the reference electrode and a platinum wire is used as the counter electrode. As shown in Fig. 5, the bonded device is connected at the working electrode. Figure 6 shows the interface impedance of the microelectrodes, which are soaked in a 0.9% NaCl solution (saline) at room temperature.

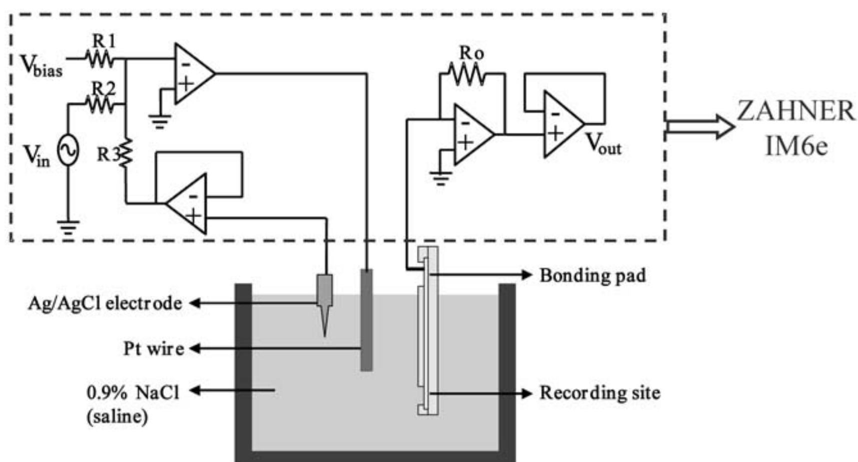

Fig. 5. Schematic diagram of impedance analyzer.

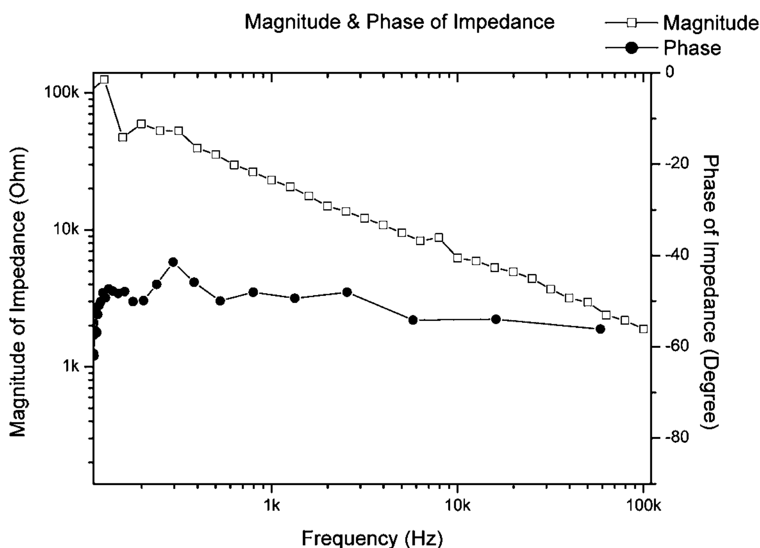

Fig. 6. Interface impedances and phase shift of microelectrodes over frequency range from 1 Hz to 100 kHz.

The sweeping frequency ranges from 1 Hz to 100 kHz. The impedance is measured with a geometric area of 900 μm^2 and has a magnitude of 371 kΩ at 1 kHz. The phase of the microelectrode is –56.2° at 1 kHz, which represents the pure capacitor behavior of the fabricated microelectrode.

In addition, an injection test with 1% agarose gel is performed to verify the functionality of the microchannels. The device is bonded with a PDMS fluid chip, and then the bonded chip was connected with a syringe through a pipette tip. Figure 7 shows the process of injecting rhodamine B (Sigma, USA) solution into 1% agarose gel through the microchannels of the device bonded with the PDMS fluid chip. The syringe is manipulated without any mechanical pump. Rhodamine B solution is easily injected into the 1% agarose gel and stains the 1% agarose gel around the device shanks, as shown in Fig. 7(b). This shows that a chemical stimulator can be successfully delivered to target cells through the microchannels.

5. Conclusion

A multifunctional neural probe is developed, which can deliver chemicals to a neuron and record the response of the neuron with spatial resolution at the cellular level. The probe contains in-plane shanks with buried microchannels and low-impedance microelectrodes fabricated using a roughened polysilicon process. Our process has advantages in that there are no limitations for the length of a shank and the depth and location of buried microchannels. The roughened polysilicon process is simple and reproducible for CMOS-compatible and low-impedance microelectrodes. The probe has three 3-mm-long shanks with 10-μm-diameter microchannels and six 30 μm × 30 μm gold microelectrodes per shank. The impedance magnitude and the phase shift of the microelectrodes are 317 kΩ and –56.2° at 1 kHz, respectively. Injection tests show that the microchannels can be used as a drug delivery pathway.

Although the fabricated device has only one reservoir, a simple mask design change in the number of reservoirs and the shape of microchannels enables the fabrication of a multi-drug-delivery probe. In addition, other electrode materials such as platinum and iridium can be used as a material in the roughened polysilicon process.

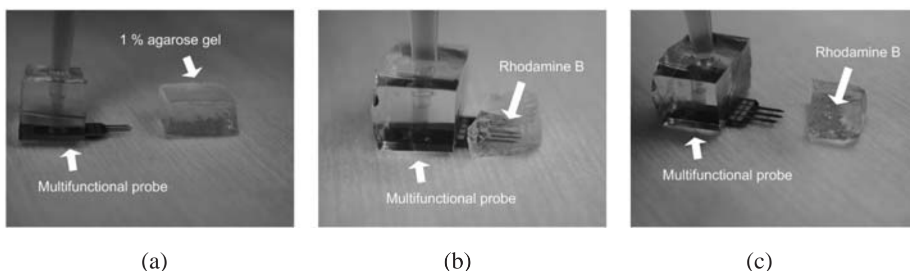

Fig. 7. Injection test with 1% agarose gel. (a) Before insertion of the multifunctional probe into 1% agarose gel. (b) Injection of rhodamine B solution into 1% agarose gel throgh microchannels; (c) Injected rhodamine B solution stains the 1% agarose gel around the multifunctional probe shanks.

Acknowledgments

This work is supported by the Nano Bioelectronics and Systems Research Center (ERC-NBS) of the Korea Science and Engineering Foundation at Seoul National University.

References

1 S. Paik, J. Kim, S. Park, S. Kim, K. Chun, J. Chang and D. Cho: Proceedings of International Sensor Conference (Seoul, 2001) p. 97.
2 S. Paik, J. Kim, S. Park, S. Kim, K. Chun, J. Chang and D. Cho: Proceedings of Pacific Rim Workshop on Transducers and Micro/Nano Technologies (Xiamen, 2002) p. 725.
3 S. Paik and D. Cho: Journal of the Korean Physical Society **41** (2002) 1046.
4 S. Paik, Y. Park and D. Cho: IOP Journal of Micromechanics and Microengineering **13** (2003) 373.
5 S. Paik, J. Lim, I. Jung, Y. Park, S. Byun, S. Chung, K. Chun, J. Chang and D. Cho: Proceedings of Transducers 2003: 12th International Conference on Solid State Sensors and Actuators (Boston, 2003) p. 1446.
6 D. Borkholder, Ph.D. Thesis, Department of Electrical Engineering, Stanford University (1998).
7 J. Chen and K.D. Wise: Trans. Electron. Devices **44** (1997) 1401.
8 J. Chen and K.D. Wise: Proceedings of the 8th International Conference on Solid State Sensors and Actuators, and Eurosensors IX (Transducers'95), Technical Digest (Stockholm, 1995) p. 321.
9 D. Borkholder, J. Bao, N. Maluf, E. Perl and G. Kovacs: J. Neurosci. Methods **77** (1997) 61.
10 W. Regehr, J. Pine and D. Rutledge: IEEE Trans. Biomed. Eng. **35** (1998) 1023.
11 S. Mailley, M. Hyland, P. Mailley, J. McLaughlin and E. McAdams: Mater. Sci. Eng. C **21** (2002) 167.
12 G. Kovacs, C. Storment, M. Halks-Miller, C. Belczynski, C. Santina, E. Lewis and N. Maluf: IEEE Trans. Biomed. Eng. **41** (1994) 567.
13 T. Akin, K. Najafi, R. Smoke and R. Bradley: IEEE Trans. Biomed. Eng. **41** (1994) 305.
14 B. Ziaie, Y. Gianchandani and K. Najafi: Proc. of Dig. Tech. Papers Int. Conf. Solid-State Sensors and Actuators, Transducers'91 (San Francisco, 1991) p. 124.
15 H. Sugihara, M. Taketani and T. Mitsumata: United States Patent 5810725 (1998).
16 C. Kim and K. Wise: IEEE J. Solid-State Circuits **31** (1996) 1230.
17 J. Weiland and D. Anderson: IEEE Trans. Biomed. Eng. **47** (2000) 911.
18 X. Cui, J. Hetke, J. Wiler, D. Anderson and D. Martin: Sensors Actuators A **93** (2001) 8.
19 X. Beebe and T. Rose: IEEE Trans. Beiomed. Eng. **35** (1998) 494.
20 J. Weiland, S. Cogan and M. Humayun: Proc. 1st Joint BMES/EMBS Conf. (Atlanta, 1999) p. 378.
21 M. Gingerich, J. Wiler and K. Wise: Proc. 1st Joint BMES/EMBS Conf. (Atlanta, 1999) p. 471.
22 D. Anderson, K. Najafi, S. Tanghe, D. Evans, K. Levy, J. Hetke, X. Xue, J. Zappia and K. Wise: IEEE Trans. Biomed. Eng. **36** (1989) 693.
23 I. Lee, C. Whang, K. Choi, M. Choo and Y. Lee: Biomaterials **23** (200) 2375.
24 T. Kamins: Polycrystalline Silicon for Integrated Circuit Applications (Boston, Kluwer 1998)
25 S. Lee, S. Yi and D. Cho: J. Kor. Phys. Soc. **35** (1999) S1106
26 S. Lee, C. Cho, J. Kim, S. Park, S. Yi, J. Kim and D. Cho: J. Micromech. Microeng. **8** (1998) 330
27 S. Lee, C. Cho, J. Kim, S. Park, S. Yi, D. Cho and J. Kim: J. Kor. Phys. Soc. **33** (1998) S392.